Nuclear Physics B182 (1981) 397–426

QCD CORRECTIONS FOR TWO-JET PRODUCTION IN PHOTON-PHOTON COLLISIONS

F A BERENDS[1] and Z KUNSZT[2]

Deutsches Elektronen-Synchrotron DESY, Hamburg, Germany

R. GASTMANS[3]

Instituut voor Theoretische Fysica, University of Leuven, B-3030 Leuven, Belgium

Received 22 September 1980

We present the calculation of the first-order QCD corrections to the process $\gamma\gamma \to q\bar{q}$, including virtual gluons and bremsstrahlung of soft and hard collinear gluons The obtained cross section is then used to calculate the α_s corrections to the process $e^+e^- \to e^+e^- + 2$ jets The numerical importance of hard acollinear gluons is also discussed

1. Introduction

Photon-photon collisions constitute an important class of phenomena produced by e^+e^- collisions in electron storage rings. They have cross sections which increase with energy in contradistinction with the cross sections in the annihilation channel [1]. For the study of hadronic processes, they are extremely useful as they provide information about the C-even states. Moreover, they allow one in principle to measure properties of quarks which are inaccessible in e^+e^- annihilation. Perhaps the most important quantity in this respect is the sum of the quark charges to the fourth power, $R_{\gamma\gamma}$. It is obtained (in the framework of the asymptotically free parton model) by a measurement of the cross section for $e^+e^- \to e^+e^- + 2$ jets, where the jets have large transverse momenta. In the process $e^+e^- \to \gamma^* \to 2$ jets, one measures the sum of the quark charges to the second power, R_γ, but the complementary information of $R_{\gamma\gamma}$ is important for distinguishing among different quark models.

Another reason for studying the process $e^+e^- \to e^+e^- + 2$ jets is that it is predicted to have the largest cross section of all the different jet cross sections in photon-photon collisions [2]. Furthermore, it provides a test of the $\not{p}^{-1}$ behavior of the quark propagator, at least in its lowest order description.

[1] Permanent address: Instituut-Lorentz, University of Leiden, The Netherlands.
[2] Permanent address: Eötvös University, Budapest, Hungary
[3] Onderzoeksleider, NFWO, Belgium.

However, one knows that QCD can sometimes lead to large one-loop corrections. It is therefore important to know whether this reaction would also suffer from this evil, in which case a precise determination of $R_{\gamma\gamma}$ would not be very straightforward.

This paper presents the calculation of $e^+e^- \to e^+e^- + 2$ jets up to order α_s. In a previous letter [3], we gave the results of the calculation, but in view of the extensive computations which underly them, we think it is worthwhile to present their derivation in more detail. Also, in ref. [3] we did not discuss the numerical importance of the hard acollinear gluon emission, which one must know in order to extract $R_{\gamma\gamma}$ from the data.

As described in ref. [2], to obtain the cross section for $e^+e^- \to e^+e^- + 2$ jets, one first calculates the cross section for the subprocess $\gamma\gamma \to q\bar{q}$, which is then folded with the equivalent photon spectra, approximately given by

$$N(x) = \left(\frac{\alpha}{2\pi} \ln \eta\right) \frac{1 + (1-x)^2}{x}, \tag{1.1}$$

where

$$\eta = \begin{cases} s/4m_e^2, & \text{no tagging,} \\ \theta_{\max}^2/\theta_{\min}^2, & \text{tagging of electrons.} \end{cases} \tag{1.2}$$

Here, $s = 4E^2$, E is the beam energy, m_e the electron mass, and $[\theta_{\min}, \theta_{\max}]$ the angular range in the e^+e^- c.m. frame in which the electrons can be detected.

In sect. 2, we first derive the lowest order cross section for the subprocess. We then show how the folding with the equivalent photon spectra (1.1) can be performed, following the methods of appendix A in ref. [2]. In this way, we obtain the integrated cross section for jets with a trigger momentum larger than some minimum value. Sect. 3 presents the calculation of the virtual gluon correction, as well as the bremsstrahlung of soft and hard collinear gluons. We derive these formulae using dimensional regularization [4] as well infinitesimal mass regularization and list the different contributions separately. For completeness, we also list the analogous expressions which are useful for e^+e^- annihilation. Finally, we present the result for the corresponding integrated cross section, which can be seen as an analogue for $\gamma\gamma$ collisions of the Sterman-Weinberg [5] formula e^+e^- annihilation. In sect. 4, we give the formula for hard acollinear gluon bremsstrahlung and discuss its numerical importance. Finally, in sect. 5, we give our conclusions.

2. Lowest order results

From sect. 1 it is clear that we have to know first the cross section for the subprocess $\gamma\gamma \to q\bar{q}$. In the lowest order, we have to consider the two Feynman

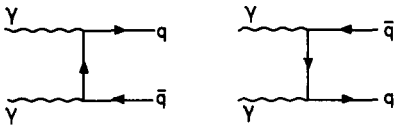

Fig 1 Lowest order Feynman diagrams for $\gamma\gamma \to q\bar{q}$

diagrams of fig. 1. They lead to the cross section

$$\frac{d\sigma^0}{d\hat{t}} = \frac{2\pi\alpha^2}{\hat{s}^2} 3e_q^4 \left(\frac{\hat{t}}{\hat{u}} + \frac{\hat{u}}{\hat{t}} \right), \tag{2.1}$$

where $\hat{s}$, $\hat{t}$, and $\hat{u}$ are the Mandelstam variables for the subprocess, and e_q is the fractional charge of the quark. We assume that all particles are ultrarelativistic, and we neglect masses whenever possible.

To obtain the jet cross section for $e^+e^- \to e^+e^- + 2$ jets (see fig. 2), we follow the methods of appendix A in ref. [2]. One parametrizes the equivalent photon spectrum and the cross section for the subprocess as follows:

$$xN(x) = \Lambda(1-x)^{g_a},$$

$$\frac{d\sigma^0}{d\hat{t}} = \pi D \hat{s}^{-2} \hat{x}_t^{-T} \hat{x}_u^{-U}. \tag{2.2}$$

Hence

$$\Lambda = \frac{\alpha}{2\pi} \ln\eta,$$

$$g_a = 0 \text{ or } 2,$$

$$D = 2\alpha^2 \left(3e_q^4\right),$$

$$T = -1, U = +1 \quad \text{or} \quad T = +1, U = -1, \tag{2.3}$$

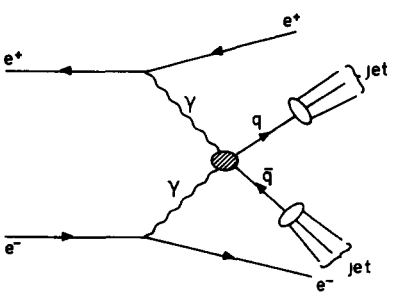

Fig 2 Feynman diagram for $e^+e^- \to e^+e^-\gamma\gamma \to e^+e^- + 2$ jets

as, by definition

$$\hat{x}_t = -\hat{t}/\hat{s}, \qquad \hat{x}_u = -\hat{u}/\hat{s}. \tag{2.4}$$

Denoting the jet four-momentum by $p = (E, \boldsymbol{p})$, one introduces the variables

$$\varepsilon = 1 - \frac{2|\boldsymbol{p}|}{\sqrt{s}}, \qquad x_F = \frac{2p_z}{\sqrt{s}}, \tag{2.5}$$

which are defined in the e^+e^- c.m. frame. The differential jet cross section is then

$$E\frac{d\sigma}{d^3p} = \frac{\varepsilon^{1+g_a+g_b}}{p_\perp^4} D\Lambda^2 \int_0^1 dy\, y^{g_a}(1-y)^{g_b} \hat{x}_u^{1-U-g_a} \hat{x}_t^{1-T-g_b}, \tag{2.6}$$

with $p_\perp$ the jet momentum perpendicular to the beam axis, and

$$\hat{x}_t = \tfrac{1}{2}(1 - x_F + \varepsilon) - \varepsilon y,$$

$$\hat{x}_u = \tfrac{1}{2}(1 + x_F - \varepsilon) + \varepsilon y. \tag{2.7}$$

We find it advantageous to introduce new variables, u, v, and z, given by

$$u = \tfrac{1}{2}\left(\sqrt{x_F^2 + z} - x_F\right),$$

$$v = \tfrac{1}{2}\left(\sqrt{x_F^2 + z} + x_F\right),$$

$$uv = \tfrac{1}{4}z, \qquad \text{with } z = \left(\frac{2p_\perp}{\sqrt{s}}\right)^2, \tag{2.8}$$

and to make a change of integration variable*

$$y = (1 - v - t)/\varepsilon, \tag{2.9}$$

where $u < t < 1 - v$. Eq. (2.6) then becomes

$$E\frac{d\sigma}{d^3p} = \frac{D\Lambda^2}{p_\perp^4} \int_u^{1-v} dt \left(\frac{1-v-t}{1-t}\right)^{g_a} \left(\frac{t-u}{t}\right)^{g_b} (1-t)^{1-U} t^{1-T}. \tag{2.10}$$

If we change $t \leftrightarrow 1 - t$, $T \leftrightarrow U$, $g_a \leftrightarrow g_b$, we can also write

$$E\frac{d\sigma}{d^3p} = \frac{D\Lambda^2}{p_\perp^4} \int_v^{1-u} dt \left(\frac{1-u-t}{1-t}\right)^{g_a} \left(\frac{t-v}{t}\right)^{g_b} (1-t)^{1-U} t^{1-T}. \tag{2.11}$$

* In the notation of ref [2] u, v are x_t and x_u, respectively The quantity t equals $\hat{x}_t$

Thus, for cross sections which are $\hat{t} \leftrightarrow \hat{u}$ symmetric, it suffices to consider only half the terms in the cross section, e.g. the first one in eq. (2.1), and to write

$$E\frac{d\sigma}{d^3p} = \frac{D\Lambda^2}{p_\perp^4}\left[\int_u^{1-v} dt \left(\frac{1-v-t}{1-t}\right)^{g_a} \times \left(\frac{t-u}{t}\right)^{g_b} (1-t)^{1-U} t^{1-T} + (u \leftrightarrow v)\right]. \tag{2.12}$$

Since

$$\int_{p_\perp > \sqrt{s}\beta/2} \frac{d^3p}{E} = \tfrac{1}{2}s\pi \int_{\beta^2}^1 \frac{dz}{z^2} \int_{\sqrt{z}/2}^{(1+\sqrt{1-z})/2} \frac{dv}{v} = \tfrac{1}{2}s\pi \int_{\beta^2}^1 \frac{dz}{z^2} \int_{(1-\sqrt{1-z})/2}^{\sqrt{z}/2} \frac{du}{u}, \tag{2.13}$$

we can make use of the $u \leftrightarrow v$ symmetry of the integrand, and write for the integrated jet cross section with trigger momentum $p_\perp$ larger than some minimum value $\frac{1}{2}\beta\sqrt{s}$

$$\sigma\left(p_\perp > \tfrac{1}{2}\sqrt{s}\beta\right) = \frac{8\pi D\Lambda^2}{s} \int_{\beta^2}^1 \frac{dz}{z^2} \int_{(1-\sqrt{1-z})/2}^{(1+\sqrt{1-z})/2} \frac{dv}{v} f(v,z), \tag{2.14}$$

where

$$f(v,z) = \sum_{g_a, g_b} \int_{z/4v}^{1-v} dt \left(\frac{1-v-t}{1-t}\right)^{g_a} \left(\frac{t-z/4v}{t}\right)^{g_b} (1-t)^{1-U} t^{1-T}. \tag{2.15}$$

For our specific case, we have $T = 1$, $U = -1$ and

$$f(v,z) = \int_a^b dt \left[(1-t)^2 + (b-t)^2 + \left(1-\frac{a}{t}\right)^2 (1-t)^2 + \left(1-\frac{a}{t}\right)^2 (b-t)^2\right]$$

$$= \tfrac{4}{3}(b^3 - a^3) + 2(b-a)(1+a-b) + (b-a)(1+b^2)\frac{a}{b}$$

$$+ 2a(1+a+ab+b^2)\ln\frac{a}{b}, \tag{2.16}$$

where

$$a = z/4v, \qquad b = 1-v. \tag{2.17}$$

To perform the remaining integrals in (2.14), there is no great problem, but the calculation is rather lengthy. The integral over v can be done exactly, and for the z-integration we take $\beta \to 0$, retaining only the terms of order β^{-2} and the constant terms. We refer to appendix A for details of the calculation.

The integrated jet cross section in lowest order then becomes

$$\sigma^0(p_\perp > p_\perp^{\min}) = \frac{32\pi}{3}\alpha^2 R_{\gamma\gamma}\left(\frac{\alpha}{2\pi}\ln\eta\right)^2 \frac{1}{(p_\perp^{\min})^2}$$

$$\times\left\{\rho - \tfrac{14}{3} + \frac{(p_\perp^{\min})^2}{2s}\left[\rho^3 + \left(\tfrac{51}{2} - \pi^2\right)\rho + 12\zeta(3) - \tfrac{33}{2}\right]\right.$$

$$\left. + O\left(\frac{(p_\perp^{\min})^4}{s^2}\right)\right\}, \tag{2.18}$$

where

$$\rho = \ln\left[\frac{s}{(p_\perp^{\min})^2}\right],$$

$$R_{\gamma\gamma} = 3\sum_{q=u,d,s,c} e_q^4 = \tfrac{34}{27}, \tag{2.19}$$

and $\zeta(3) = 1.202$ is Riemann's zeta-function of argument 3.

One comment should be made concerning this result. In ref. [2], the photon spectra terms $1 + (1-x)^2$ were approximated by 2, and, as a result, these authors obtain $-\frac{19}{6}$ instead of $-\frac{14}{3}$ for the second term in the curly bracket (they did not calculate the remaining terms). We find that by taking the complete expression (1.1) for the photon spectrum, it becomes necessary to calculate also the terms of order s^{-1} to obtain sensible results. Indeed, for $\sqrt{s} = 30$ GeV and $p_\perp^{\min} = 4$ GeV, the terms $\rho - \frac{14}{3}$ alone would have given a negative cross section. Now, we find that jets with $p_\perp > 4$ GeV contribute 0.2 units of R to the e^+e^- total cross section for $\sqrt{s} = 30$ GeV from this lowest order process.

3. Second-order results

In this section, we calculate successively the virtual gluon corrections of order α_s to $e^+e^- \to e^+e^- + 2$ jets, the soft gluon bremsstrahlung contribution, and the hard collinear gluon correction.

3 1 VIRTUAL GLUON CORRECTIONS

We consider first the cross section to order α_s for $\gamma\gamma \to q\bar{q}$, which means evaluating the eight Feynman diagrams of fig. 3. We shall present the calculation in the Landau gauge, but later on we shall quote our results in the Feynman gauge as well. In the Landau gauge, the gluon propagator has the form

$$D_{\mu\nu}^{ab} = -i\frac{g_{\mu\nu} - k_\mu k_\nu/k^2}{k^2 + i\varepsilon}\delta_{ab}, \tag{3.1}$$

and, for massless quarks, the quark self-energy vanishes at the one-loop level [6]. The Ward identity then implies that the vertex corrections must not be renormalized.

It is well-known that in dealing with massless quarks and gluons one must regularize ultraviolet divergences as well as infrared divergences and mass singularities. We find it convenient to use the continuous dimension method to regularize them all [4,6,7]. The amplitudes at the one-loop level can then develop a double pole structure in $n-4$, where n is the continuous dimension parameter.

For the vertex correction (fig. 4), we have

$$\Lambda_\mu(p',p) = -\frac{i\alpha_s}{4\pi^3} \times \int d^4k \frac{\gamma^\alpha(\not{p}' - \not{k})\gamma_\mu(\not{p} - \not{k})\gamma^\beta}{k^2(p'-k)^2(p-k)^2}\left(g_{\alpha\beta} - \frac{k_\alpha k_\beta}{k^2}\right), \tag{3.2}$$

but for our applications, the photon and one of the quarks is on the mass-shell, which considerably simplifies the calculation. For $p'^2 = 0$, we find with the standard methods

$$\bar{u}(p')\Lambda_\mu(p',p) = \frac{\alpha_s}{2\pi}\left[\frac{2}{n-4} + 2\ln(-p^2\pi) + 2\gamma - \tfrac{5}{2}\right] \times \bar{u}(p')\left[\gamma_\mu - 2p_\mu \not{p}/p^2\right], \tag{3.3}$$

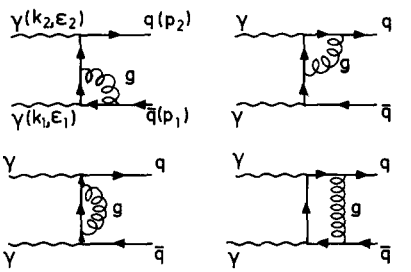

Fig 3 Virtual gluon corrections of order α_s for $\gamma\gamma \to q\bar{q}$ The solid lines represent quarks, the wavy lines photons, and the curly ones gluons

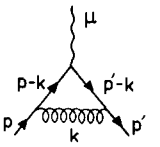

Fig 4 Vertex correction

where γ is Euler's constant, and for $p^2 = 0$,

$$\Lambda_\mu(p',p)v(p) = \frac{\alpha_s}{2\pi}\left[\frac{2}{n-4} + 2\ln(-p'^2\pi) + 2\gamma - \tfrac{5}{2}\right] \times \left[\gamma_\mu - 2p'_\mu \not{p}'/p'^2\right] v(p). \tag{3.4}$$

Consequently, the two vertex correction diagrams of fig. 3 have amplitudes given by (e denotes the quark charge)

$$M^1 = -ie^2\frac{\alpha_s}{2\pi}\left[\frac{2}{n-4} + 2\ln(-\hat{t}\pi) + 2\gamma - \tfrac{5}{2}\right] \times \frac{1}{\hat{t}}\bar{u}(p_2)\left[\not{\varepsilon}_2(\not{p}_2 - \not{k}_2)\not{\varepsilon}_1 + 2\not{\varepsilon}_2 p_1\cdot\varepsilon_1\right] v(p_1),$$

$$M^2 = -ie^2\frac{\alpha_s}{2\pi}\left[\frac{2}{n-4} + 2\ln(-\hat{t}\pi) + 2\gamma - \tfrac{5}{2}\right] \times \frac{1}{\hat{t}}\bar{u}(p_2)\left[\not{\varepsilon}_2(\not{p}_2 - \not{k}_2)\not{\varepsilon}_1 - 2\not{\varepsilon}_1 p_2\cdot\varepsilon_2\right] v(p_1), \tag{3.5}$$

with $\hat{t} = (p_2 - k_2)^2$. Taking into account also the crossed diagrams and interfering them with the lowest order amplitudes, we get the following correction due to the vertex corrections:

$$\delta_{\text{vertex}} = \frac{4\alpha_s}{3\pi}\left[\frac{1}{n-4}\left(\frac{-\hat{8}\hat{u}\hat{t}}{\hat{t}^2+\hat{u}^2}\right) + \frac{2\hat{u}\hat{t}}{\hat{t}^2+\hat{u}^2} \times \left(-\ln(-\hat{t}\pi) - \ln(-\hat{u}\pi) - 2\gamma + 5\right)\right], \tag{3.6}$$

where all contributions to the cross section in second order are written as

$$\frac{d\sigma^1}{d\Omega} = \frac{d\sigma^0}{d\Omega}\delta. \tag{3.7}$$

Note the inclusion of the color factor $\frac{4}{3}$ in eq. (3.6).

For the box diagrams, the calculations proceed similarly; e.g., the fourth diagram of fig. 3 is given by

$$M^4 = -e^2 \frac{\alpha_s}{4\pi^3} \int d^4k \frac{\bar{u}(p_2)\gamma^\alpha(\not k + \not k_2)\not\epsilon_2 \not k \not\epsilon_1(\not k - \not k_1)\gamma^\beta v(p_1)}{k^2(k+k_2)^2(k-k_1)^2(k-k_1+p_1)^2}$$

$$\times \left[g_{\alpha\beta} - (k-k_1+p_1)_\alpha (k-k_1+p_1)_\beta / (k-k_1+p_1)^2 \right]. \qquad (3.8)$$

This time, however, we have an infrared divergence as well as mass singularities to deal with, resulting in a double pole structure for the amplitude. The calculation is more lengthy than in the case of the vertex correction, and we made use of the symbolic manipulation program REDUCE [8] to calculate the traces in n dimensions. The explicit result for the box diagrams can be found in table 1.

3.2 SOFT GLUON BREMSSTRAHLUNG

For experimental situations, the one-quark state is degenerate with a state composed of one quark and soft gluons. To order α_s, this means we have to calculate

TABLE 1
The various corrections to $\gamma\gamma \to q\bar{q}(g)$ in the Landau gauge with the continuous dimension regularization method

$\frac{3\pi}{4\alpha_s}\delta$	$(n-4)^{-2}$	$(n-4)^{-1}$	Finite terms
$\frac{3\pi}{4\alpha_s}\delta_{\text{vertex}}$		$\frac{-8ut}{t^2+u^2}$	$\frac{2ut}{t^2+u^2}\left[-\ln(ut\pi^2) - 2\gamma + 5\right]$
$\frac{3\pi}{4\alpha_s}\delta_{\text{box}}$	-4	$-2\ln(s\pi) - 2\gamma + 3 + \frac{8ut}{t^2+u^2}$	$-\frac{1}{2}[\ln(s\pi)+\gamma]^2 - \frac{7}{2} + \frac{7}{12}\pi^2 + \frac{1}{t^2+u^2} \times \left[\left(t^2+ut+\frac{1}{2}u^2\right)\ln^2\left(\frac{s}{-t}\right) + u\left(t-2s-\frac{1}{2}u\right) \times (\ln(-t\pi)+\gamma) - ut(\ln(s\pi)+\gamma) - 5ut + (t \leftrightarrow u)\right]$
$\frac{3\pi}{4\alpha_s}\delta_{\text{soft}}$	4	$2[\ln(16\varepsilon^2E^2\pi)+\gamma]$	$\frac{1}{2}[\ln(16\varepsilon^2E^2\pi)+\gamma]^2 - \frac{1}{4}\pi^2$
$\frac{3\pi}{4\alpha_s}\delta_{\text{hard}}$		$-4\ln 2\varepsilon - 3$	$(\ln 2\delta + \frac{1}{2}\ln\pi + \frac{1}{2}\gamma)(-4\ln 2\varepsilon - 3) - 2\ln^2 2\varepsilon - 4\ln E \ln 2\varepsilon - 3\ln E - \frac{2}{3}\pi^2 + \frac{13}{2}$

By s, t, u we mean, in fact, the quantities $\hat{s}$, $\hat{t}$, $\hat{u}$ as defined in the text.

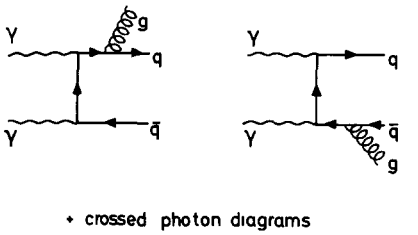

Fig 5 Feynman diagrams for soft gluon corrections

the cross section corresponding to fig. 5, with the constraint that the gluon energy k be smaller than some cut-off value $2\varepsilon E \ll E$, E being the energy of the incoming photons in their c.m. frame. It is well known that in this case the soft gluon matrix element is proportional to the purely elastic cross section and that the correction factor for massless quarks is given by

$$\delta_s = \frac{\alpha_s}{3\pi^2} 2p_1\cdot p_2 \int_{k<2\varepsilon E} d^3k \frac{1}{k(p_1\cdot k)(p_2\cdot k)}. \tag{3.9}$$

The gluon being soft, we have an infrared divergence in eq. (3.9), and, the quarks being massless, we have an additional mass singularity. Hence, in the continuous dimension method, we must expect a double pole structure for δ_s. Indeed, in n dimensions,

$$\delta_s = \frac{4\alpha_s}{3\pi^2} \frac{2\pi^{n/2-1}}{\Gamma(\frac{1}{2}n-1)} \int_0^{\pi} d\theta \sin^{n-5}\theta \int_0^{2\varepsilon E} dk\, k^{n-5}, \tag{3.10}$$

where the factor $2\pi^{n/2-1}/\Gamma(\frac{1}{2}n-1)$ comes from the integration over the angular variables which do not appear in the integrand. We chose $p_1\cdot k = Ek(1-\cos\theta)$ and $p_2\cdot k = Ek(1+\cos\theta)$. Expanding around $n=4$, we find for the soft gluon correction

$$\delta_s = \frac{4\alpha_s}{3\pi}\left\{\frac{4}{(n-4)^2} + \frac{2}{n-4}\left[\ln(16\varepsilon^2E^2\pi)+\gamma\right]\right.$$

$$\left. + \tfrac{1}{2}\left[\ln(16\varepsilon^2E^2\pi)+\gamma\right]^2 - \tfrac{1}{4}\pi^2\right\}. \tag{3.11}$$

3 3 HARD COLLINEAR GLUON BREMSSTRAHLUNG

Not only the emission of soft gluons leads to an experimental degeneracy, but also the bremsstrahlung of hard gluons in a direction which is sufficiently parallel to the quark or antiquark direction. In practice, this means we also have to calculate the cross section corresponding to the Feynman diagrams of fig. 6 with the constraints that the gluon energy k lie in the range $2\varepsilon E < k < E$, $\varepsilon \ll 1$, and that $\sphericalangle(\boldsymbol{k},\boldsymbol{p}_1)$ or $\sphericalangle(\boldsymbol{k},\boldsymbol{p}_2)$ be smaller than 2δ, $\delta \ll 1$. Again, $p_1(p_2)$ is the antiquark (quark) four-momentum.

The matrix elements for the six Feynman diagrams are, omitting color matrices for simplicity,

$$M_1 = \frac{-ie^2 g}{4k\cdot p_2 k_1\cdot p_1}\bar{u}(p_2)\not{\varepsilon}(\not{p}_2+\not{k})\not{\varepsilon}_2(\not{p}_1-\not{k}_1)\not{\varepsilon}_1 v(p_1),$$

$$M_2 = \frac{-ie^2 g}{4k_1\cdot p_1 k_2\cdot p_2}\bar{u}(p_2)\not{\varepsilon}_2(\not{p}_2-\not{k}_2)\not{\varepsilon}(\not{k}_1-\not{p}_1)\not{\varepsilon}_1 v(p_1),$$

$$M_3 = \frac{-ie^2 g}{4k\cdot p_1 k_2\cdot p_2}\bar{u}(p_2)\not{\varepsilon}_2(\not{p}_2-\not{k}_2)\not{\varepsilon}_1(\not{k}+\not{p}_1)\not{\varepsilon} v(p_1),$$

$$M_4 = \frac{-ie^2 g}{4k\cdot p_2 k_2\cdot p_1}\bar{u}(p_2)\not{\varepsilon}(\not{p}_2+\not{k})\not{\varepsilon}_1(\not{p}_1-\not{k}_2)\not{\varepsilon}_2 v(p_1),$$

$$M_5 = \frac{-ie^2 g}{4k_2\cdot p_1 k_1\cdot p_2}\bar{u}(p_2)\not{\varepsilon}_1(\not{p}_2-\not{k}_1)\not{\varepsilon}(\not{k}_2-\not{p}_1)\not{\varepsilon}_2 v(p_1),$$

$$M_6 = \frac{-ie^2 g}{4k\cdot p_1 k_1\cdot p_2}\bar{u}(p_2)\not{\varepsilon}_1(\not{p}_2-\not{k}_1)\not{\varepsilon}_2(\not{k}+\not{p}_1)\not{\varepsilon} v(p_1), \tag{3.12}$$

where g is the gauge coupling constant ($g^2/4\pi = \alpha_s$), and ε_μ is the polarization vector of the gluon.

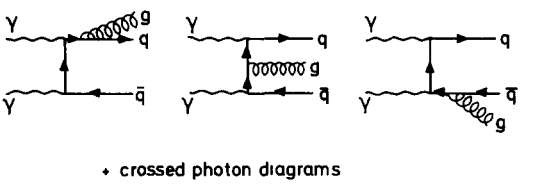

Fig 6 Feynman diagrams for hard collinear gluon corrections

For the case when k is almost parallel to p_1, only the diagrams M_3 and M_6 lead to singularities, hence, for the cross section, we only have to integrate

$$F_1 = \sum \left[|M_3|^2 + 2\,\mathrm{Re} M_3^* (M_1 + M_2 + M_4 + M_5 + M_6) \right.$$

$$\left. + |M_6|^2 + 2\,\mathrm{Re} M_6^* (M_1 + M_2 + M_4 + M_5) \right], \tag{3.13}$$

where the summation extends over the polarization states of the photons, the gluon, and the quarks.

In the continuous dimension method, the gluon has to be treated in n dimensions, and we made again use of REDUCE [8] to calculate the traces. We thus obtain

$$F_1 = \frac{2e^4 g^2 \hat{s}'}{k\cdot p_1 k\cdot p_2} \left[2\frac{\hat{t}^2 + \hat{u}^2}{\hat{t}'\hat{u}'} + (n-4)\left(\frac{(\hat{t}-\hat{u})^2}{\hat{t}'\hat{u}'} + 2 - \frac{\hat{t}}{\hat{u}'} - \frac{\hat{u}}{\hat{t}'} \right) \right.$$

$$\left. + (\hat{t} \leftrightarrow \hat{t}', \hat{u} \leftrightarrow \hat{u}') \right], \tag{3.14}$$

$$\hat{s} = (k_1 + k_2)^2, \qquad \hat{t} = (k_1 - p_1)^2, \qquad \hat{u} = (k_1 - p_2)^2,$$

$$\hat{s}' = (p_1 + p_2)^2, \qquad \hat{t}' = (k_2 - p_2)^2, \qquad \hat{u}' = (k_2 - p_1)^2. \tag{3.15}$$

Averaging this matrix element squared over the photon polarizations, summing over the color, and integrating over the gluon phase space with the stated restrictions, we have for the cross section

$$\frac{d\sigma^{\mathrm{H1}}}{d\Omega} = \frac{2\alpha^2 \alpha_s e_q^4}{\hat{s}\pi} \frac{1+\cos^2\theta}{\sin^2\theta} \left\{ \frac{1}{n-4}(-4\ln 2\varepsilon - 3) + \left(\ln 2\delta + \tfrac{1}{2}\ln\pi + \tfrac{1}{2}\gamma\right)(-4\ln 2\varepsilon - 3) \right.$$

$$\left. - 2\ln^2 2\varepsilon - 4\ln 2\varepsilon \ln E - 3\ln E - \tfrac{2}{3}\pi^2 + \tfrac{13}{2} \right\}, \tag{3.16}$$

where θ is the polar angle of the quark in the photon c.m. frame.

For the case where the gluon is emitted almost parallel to the quark, we find an identical cross section; hence, for hard collinear gluon bremsstrahlung, we have a correction

$$\delta_H = \frac{4\alpha_s}{3\pi}\left[\frac{1}{n-4}(-4\ln 2\varepsilon - 3) + (\ln 2\delta + \tfrac{1}{2}\ln\pi + \tfrac{1}{2}\gamma)(-4\ln 2\varepsilon - 3)\right.$$

$$\left. - 2\ln^2 2\varepsilon - 4\ln 2\varepsilon \ln E - 3\ln E - \tfrac{2}{3}\pi^2 + \tfrac{13}{2}\right]. \tag{3.17}$$

3.4 THE JET CROSS SECTION

Adding up the corrections due to virtual and real gluons (soft and hard collinear ones), we see that the various double and single poles cancel, and we obtain an extra contribution to the cross section for the subprocess $\gamma\gamma \to q\bar{q}(g)$ to order α_s, i.e.

$$\frac{d\sigma^1}{d\Omega} = \frac{d\sigma^0}{d\Omega}\delta_T, \tag{3.18}$$

with

$$\delta_T = \frac{4\alpha_s}{3\pi}\left\{-\ln\delta(4\ln 2\varepsilon + 3) - \tfrac{1}{3}\pi^2 + 3\right.$$

$$\left. + \frac{1}{2(\hat{t}^2 + \hat{u}^2)}\left[(\hat{s}^2 + \hat{t}^2)\ln^2\left(\frac{\hat{s}}{-\hat{t}}\right) + \hat{u}(2\hat{s} - \hat{u})\ln\left(\frac{\hat{s}}{-\hat{t}}\right) + (\hat{t} \leftrightarrow \hat{u})\right]\right\}. \tag{3.19}$$

This formula can be viewed as an analogue for photon-photon collisions of the Sterman-Weinberg formula [5] for $e^+e^- \to \gamma^* \to 2$ jets. Note that the same $\ln\delta$ dependence is obtained, as it is a universal factor associated with soft and hard collinear gluon bremsstrahlung from quarks.

With the same techniques as in sect. 2, we can now evaluate the jet cross section to order α_s, using the cross section for the subprocess to order α_s. This time, however, the calculations are much more involved because the appearance of extra log factors in eq. (3.19) introduces higher order polylogarithmic integrals. Still, the result can be expressed in terms of various powers of π and Riemann's zeta-function $\zeta(3)$. We find

for the extra contribution to $\sigma(p_\perp > p_\perp^{\min})$:

$$\sigma^1(p_\perp > p_\perp^{\min}) = \tfrac{32}{3}\pi\alpha^2 R_{\gamma\gamma}\left(\frac{\alpha}{2\pi}\ln\eta\right)^2 \frac{1}{(p_\perp^{\min})^2}$$

$$\times \frac{4\alpha_s}{3\pi}\left\{\left[\rho - \tfrac{14}{3} + \frac{(p_\perp^{\min})^2}{2s}\left(\rho^3 + \left(\tfrac{51}{2} - \pi^2\right)\rho + 12\zeta(3) - \tfrac{33}{2}\right)\right]\right.$$

$$\times\left[-\ln\delta(4\ln 2\varepsilon + 3)\right] + \left(\tfrac{53}{18} - \tfrac{1}{3}\pi^2\right)\rho - \tfrac{799}{36} + \tfrac{16}{9}\pi^2 + 4\zeta(3)$$

$$+ \frac{(p^{\min})^2}{2s}\left[\tfrac{1}{20}\rho^5 - \tfrac{1}{8}\rho^4 + \left(\tfrac{19}{4} - \tfrac{1}{3}\pi^2\right)\rho^3 + \left(6\zeta(3) - \tfrac{69}{8}\right)\rho^2\right.$$

$$\left.\left. + \left(\tfrac{219}{2} - 12\pi^2 + 15\zeta(3) - \tfrac{1}{6}\pi^4\right)\rho + 26.1\right] + O\left(\frac{(p_\perp^{\min})^4}{s^2}\right)\right\}$$

$$= \tfrac{32}{3}\pi\alpha^2 R_{\gamma\gamma}\left(\frac{\alpha}{2\pi}\ln\eta\right)^2 \frac{1}{(p_\perp^{\min})^2}\frac{\alpha_s}{\pi}$$

$$\times\left\{\left[1.333\rho - 6.222 + \frac{(p_\perp^{\min})^2}{s}(0.667\rho^3 + 10.42\rho - 1.384)\right]\right.$$

$$\times\left[-\ln\delta(4\ln 2\varepsilon + 3)\right] - 0.461\rho + 0.213 + \frac{(p_\perp^{\min})^2}{s}$$

$$\times\left[0.0333\rho^5 - 0.0833\rho^4 + 0.973\rho^3 - 0.942\rho^2 - 4.759\rho + 17.4\right]$$

$$\left. + O\left(\frac{(p_\perp^{\min})^4}{s^2}\right)\right\}. \tag{3.20}$$

The quantities ρ and $R_{\gamma\gamma}$ are given by eqs. (2.19).

Because of the size of this calculation, we did not attempt to calculate the last term in this result exactly (i.e. the coefficient 26.1 in the first formula or the

coefficient 17.4 in the second one). Rather, we determined it numerically, by performing the integrals numerically and by verifying that, for $p_\perp^{\min} < 0.17\sqrt{s}$, eq. (3.20) was a good approximation within 3%. Comparing eqs. (3.20) and (2.12), we note that we now have ρ^5 terms, which is two more powers of ρ than in the lowest order result. This is due to the fact that the cross section for the subprocess in higher order contains two powers of logarithms. Also note that in (3.20) the high powers of ρ are combined with small coefficients and that the signs over the various terms tend to oscillate, resulting in large cancellations. Certainly, in this calculation, a leading log approximation could not be trusted.

Due to the presence of the ε, δ terms in (3.20), it is not directly meaningful to ask for the numerical importance of this higher order result. These terms will cancel against similar contributions from hard acollinear gluon corrections, but we can disregard them temporarily and ask how important the remaining terms are. With $\alpha_s \simeq 0.3$, $p_\perp^{\min} = 4$ GeV and $s = 30$ GeV, we find that

$$\sigma^1/\sigma^0 \simeq -0.11, \tag{3.21}$$

which is not an unreasonable number for a QCD correction.

3.5 REMARKS

As a check on our calculations, we also performed them in the Feynman gauge, where the gluon propagator has the form

$$D_{\mu\nu}^{ab}(k) = -i\frac{g_{\mu\nu}}{k^2}\delta_{ab}. \tag{3.22}$$

This time, we have to consider the quark self-energy diagrams as well. We list the various corrections in this gauge in table 2, and the reader can easily verify that the same total correction is obtained.

Also one could introduce an infinitesimal gluon mass, λ, to regularize the infrared divergences and a small quark mass, μ, for the mass singularities. A gluon mass would break the gauge invariance of the theory, but the absence of a three-gluon vertex in our process makes this procedure harmless. The virtual and soft gluon corrections are then easily obtained from the analogous QED corrections for the process $e^+e^- \to \gamma\gamma(\gamma)$ [9]:

$$\delta_{\text{virtual}} + \delta_{\text{soft}} = \frac{4\alpha_s}{3\pi}\left\{\tfrac{3}{2}\ln\frac{\hat{s}}{\mu^2} + 2\ln\frac{\hat{s}}{\mu^2}\ln 2\varepsilon - 2\ln 2\varepsilon + \tfrac{1}{3}\pi^2 - \tfrac{3}{2} + \frac{1}{2(\hat{t}^2+\hat{u}^2)}\right.$$
$$\left.\times\left[(\hat{s}^2+\hat{t}^2)\ln^2\left(\frac{\hat{s}}{-\hat{t}}\right) + \hat{u}(2\hat{s}-\hat{u})\ln\left(\frac{\hat{s}}{-\hat{t}}\right) + (\hat{t}\leftrightarrow\hat{u})\right]\right\}. \tag{3.23}$$

TABLE 2
The various corrections to $\gamma\gamma \to q\bar{q}(g)$ in the Feynman gauge with the continuous dimension regularization method

$\frac{3\pi}{4\alpha_s}\delta$	$(n-4)^{-2}$	$(n-4)^{-1}$	Finite terms
$\frac{3\pi}{4\alpha_s}\delta_{\text{self-energy}}$		1	$-\frac{1}{2}+\frac{1}{t^2+u^2}\left[\frac{1}{2}u^2(\ln(-t\pi)+\gamma)+\frac{1}{2}t^2(\ln(-u\pi)+\gamma)\right]$
$\frac{3\pi}{4\alpha_s}\delta_{\text{vertex}}$		$-2-\frac{8ut}{t^2+u^2}$	$1-\frac{1}{t^2+u^2}\left[u(u+2t)(\ln(-t\pi)+\gamma)-5ut+(t\leftrightarrow u)\right]$
$\frac{3\pi}{4\alpha_s}\delta_{\text{box}}$	-4	$-2\ln(s\pi)-2\gamma+4+\frac{8ut}{t^2+u^2}$	$-\frac{1}{2}[\ln(s\pi)+\gamma]^2-4+\frac{7}{12}\pi^2+\frac{1}{t^2+u^2}\times\left[\left(t^2+ut+\frac{1}{2}u^2\right)\ln^2\left(-\frac{s}{t}\right)+u(t-2s)\times(\ln(-t\pi)+\gamma)-ut(\ln(s\pi)+\gamma)-5ut+(t\leftrightarrow u)\right]$
$\frac{3\pi}{4\alpha_s}\delta_{\text{soft}}$	4	$2[\ln(16\varepsilon^2E^2\pi)+\gamma]$	$\frac{1}{2}[\ln(16\varepsilon^2E^2\pi)+\gamma]^2-\frac{1}{4}\pi^2$
$\frac{3\pi}{4\alpha_s}\delta_{\text{hard}}$		$-4\ln 2\varepsilon-3$	$\left(\ln 2\delta+\frac{1}{2}\ln\pi+\frac{1}{2}\gamma\right)(-4\ln 2\varepsilon-3)-2\ln^2 2\varepsilon-4\ln E\ln 2\varepsilon-3\ln E-\frac{2}{3}\pi^2+\frac{13}{2}$

Performing the integral over the phase space for the hard collinear gluon, we now find

$$\delta_{\text{hard}}=\frac{4\alpha_s}{3\pi}\left\{-2\ln\frac{\hat{s}}{\mu^2}\left(\ln 2\varepsilon+\tfrac{3}{4}\right)-(4\ln 2\varepsilon+3)\ln\delta+2\ln 2\varepsilon+\tfrac{9}{2}-\tfrac{2}{3}\pi^2\right\}. \tag{3.24}$$

In the sum of (3.23) and (3.24), the $\ln\mu^2$ terms drop out, and the total correction as given by (3.19) is recovered.

The same technique can easily be applied to the rederivation of the Sterman-Weinberg formula [5] for $e^+e^- \to \gamma^* \to 2$ jets. The calculation of the various radiative corrections can be obtained by the appropriate substitutions in the e^+e^-

$\to \mu^+\mu^-(\gamma)$ formulae [10]. We simply list the results:

$$\delta_{\text{vertex}} = \frac{4\alpha_s}{3\pi}\left[-2\left(1-\ln\frac{s}{\mu^2}\right)\ln\frac{\lambda}{\mu}-\tfrac{1}{2}\ln^2\frac{s}{\mu^2}+\tfrac{3}{2}\ln\frac{s}{\mu^2}-2+\tfrac{2}{3}\pi^2\right],$$

$$\delta_{\text{soft}} = \frac{4\alpha_s}{3\pi}\left[-2\left(1-\ln\frac{s}{\mu^2}\right)\ln\frac{4\varepsilon E}{\lambda}-\tfrac{1}{2}\ln^2\frac{s}{\mu^2}+\ln\frac{s}{\mu^2}-\tfrac{1}{3}\pi^2\right],$$

$$\delta_{\text{hard}} = \frac{4\alpha_s}{3\pi}\left[2\left(1-\ln\frac{s}{\mu^2}\right)\ln 2\varepsilon-(4\ln 2\varepsilon+3)\ln\delta-\tfrac{3}{2}\ln\frac{s}{\mu^2}+\tfrac{9}{2}-\tfrac{2}{3}\pi^2\right],$$

$$\delta_{\text{T}} = \frac{4\alpha_s}{3\pi}\left[-(4\ln 2\varepsilon+3)\ln\delta+\tfrac{5}{2}-\tfrac{1}{3}\pi^2\right]. \tag{3.25}$$

In the continuous dimension method, these corrections would be

$$\delta_{\text{vertex}} = \frac{4\alpha_s}{3\pi}\left[\frac{-4}{(n-4)^2}+\frac{1}{n-4}(-2\ln(s\pi)-2\gamma+3)\right.$$
$$\left.-\tfrac{1}{2}(\ln(s\pi)+\gamma)^2+\tfrac{3}{2}\ln(s\pi)+\tfrac{3}{2}\gamma+\tfrac{7}{12}\pi^2-4\right],$$

$$\delta_{\text{soft}} = \frac{4\alpha_s}{3\pi}\left[\frac{4}{(n-4)^2}+\frac{2}{n-4}\left(\ln(16\varepsilon^2E^2\pi)+\gamma\right)+\tfrac{1}{2}\left(\ln(16\varepsilon^2E^2\pi)+\gamma\right)^2-\tfrac{1}{4}\pi^2\right],$$

$$\delta_{\text{hard}} = \frac{4\alpha_s}{3\pi}\left[\frac{1}{n-4}(-4\ln 2\varepsilon-3)+\left(\ln 2\delta+\tfrac{1}{2}\ln\pi+\tfrac{1}{2}\gamma\right)(-4\ln 2\varepsilon-3)\right.$$
$$\left.-2\ln^2 2\varepsilon-4\ln E\ln 2\varepsilon-3\ln E-\tfrac{2}{3}\pi^2+\tfrac{13}{2}\right], \tag{3.26}$$

and the same result for δ_T as in eq. (3.25) is obtained. Once one chooses a regularization scheme, δ_{soft} and δ_{hard} are the same for both processes. Note that in δ_T the π^2 term is also the same.

4. Inclusive large $p_\perp$ jet production

In this section we investigate the properties of the gluon bremsstrahlung matrix element and evaluate numerically the inclusive jet production cross section ($e^+e^- \to e^+e^-q\bar{q}(g)$, $p_\perp^{\text{jet}} > p_\perp^{\min}$).

4.1 HARD GLUON BREMSSTRAHLUNG AND MASS SINGULARITIES

The cross section of hard gluon bremsstrahlung can be obtained trivially from the $e^+e^- \to \gamma\gamma\gamma$ formula [11], with appropriate color and charge factors. Using the notation for the four-momenta

$$\gamma(k_1) + \gamma(k_2) \to \bar{q}(p_1) + q(p_2) + g(k_3),$$

the cross section for massless quarks, averaged over the initial spin and summed over color has the simple form

$$d\sigma = \frac{4\alpha^2\alpha_s}{3\hat{s}} R_{\gamma\gamma} |M|^2 \frac{1}{\pi^2} \frac{d^3p_1}{2p_1^0} \frac{d^3p_2}{2p_2^0} \frac{d^3k_3}{2k_3^0} \delta^{(4)}(k_1 + k_2 - p_1 - p_2 - k_3), \quad (4.1)$$

where

$$|M|^2 = s' \left[\frac{u_1^2 + v_1^2}{u_2 v_2 u_3 v_3} + \text{cyclic perm.} \right], \quad (4.2)$$

and $u_i = k_i \cdot p_1, v_i = k_i \cdot p_2, s' = 2p_1 \cdot p_2$. With the formulae (3.19) and (4.2) we have all the necessary information for the purpose of numerical evaluation of any $O(\alpha_s)$ correction. There is, however, a technical and a conceptual difficulty. The matrix element squared $|M|^2$ has six poles corresponding to collinear configurations when one of the $\boldsymbol{k}_i$'s is parallel with $\boldsymbol{p}_1$ or $\boldsymbol{p}_2$. The technical difficulty is given by the ε and δ dependence of formula (3.19) which will cancel against the contribution of $|M|^2$ integrated over hard acollinear configurations. The $\ln\varepsilon \ln\delta$ singularities are obtained in the limit when the gluon momentum is parallel with $\boldsymbol{p}_1$ or $\boldsymbol{p}_2$ ($u_3 \simeq 0, v_3 \simeq 0$). The cancellation of the $\ln\varepsilon \ln\delta$ terms must be performed analytically by subtracting and adding two simple pole terms. A convenient possibility is described in appendix B.

The conceptual difficulty is associated with the quark mass singularities given by the decays of the initial photons into collinear quark-antiquark pairs (u_1, u_2, v_1, or $v_2 \simeq 0$). Similar mass singularities are present in deep inelastic leptoproduction, in the Drell-Yan process, etc. Assuming the validity of the parton model, they are factorized into the wave function of the initial particles and give the Q^2 evolution or scale-breaking effects. For example with the help of integration variables E_q, $E_{\bar{q}}$ and $\cos\theta_{\bar{q}}$ for the phase-space integral, the condition $v_1 \simeq 0$ gives the relation $\cos\theta_{q\bar{q}} \simeq \cos\theta_{\bar{q}}$ or equivalently

$$E_q = \frac{2(E - E_{\bar{q}})}{2 + (-1 + \cos\theta_{\bar{q}}) E_{\bar{q}}/E}. \quad (4.3)$$

The corresponding curve on the Dalitz plot of E_q and $E_{\bar{q}}$ is given in fig. 7.

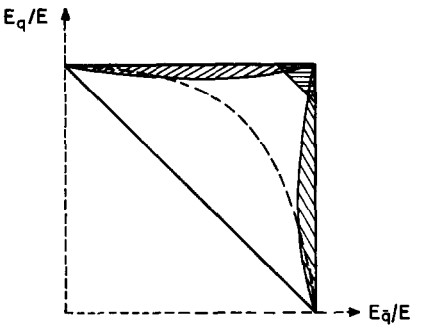

Fig 7 Dalitz plot indicating the regions of mass singularities. $v_1 \simeq 0$ is shown by the dashed curve, $u_3 \simeq 0$, $v_3 \simeq 0$ is given by the shaded area [see eq (4.2)]

Performing the integration over the momentum components of the quark, in the leading logarithmic approximation the well known Weizsäcker-Williams approximation is obtained [12, 13] (see fig. 8):

$$d\sigma_{\gamma\gamma\to q\bar{q}g} \simeq \frac{\alpha}{2\pi} \ln \frac{p_\perp^2}{M_c^2} \int dx \left[x^2 + (1-x)^2\right] d\hat{\sigma}(xk_1, k_2)_{\bar{q}\gamma\to\bar{q}g}, \qquad (4.4)$$

where M_c can be considered as either a quark mass or a momentum cut-off. The function $(\alpha/2\pi)\ln(p_\perp^2/M_c^2)[x^2+(1-x)^2]$ is the "wave function of the photon". It gives the probability that a quark is found inside the photon with momentum fraction x. This "Born approximation" of the photon wave function is modified by higher order QCD corrections. These corrections can also be calculated in the leading logarithmic approximation to all orders of α_s. The x dependence is modified but the factor $(\alpha/2\pi)\ln(p_\perp^2/M_c^2)$, of course, remains the same. The presence of this factor given by the QED vertex is a specific feature of the $\gamma\gamma$ processes. The operator product analysis of the cross section of the reaction $\gamma\gamma \to$ hadrons [13] revealed that the value of the "quark mass" parameter M_c is of the order of the QCD parameter Λ, appearing in the running coupling constant α_s.

Unfortunately the ambiguity associated with the value of the parameter M_c cannot be eliminated. The photon has also a "ρ-component", i.e. in the small $p_\perp$ region the

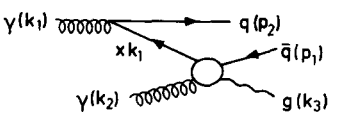

Fig 8 Diagrammatic illustration of the Weizsacker-Williams approximation [see eq (4.4)]

"photon wave function" is strongly influenced by non-perturbative effects. However, assuming the validity of the parton model, M_c is expected to have a value between 200 and 800 MeV. Such an ambiguity in the leading log approximation is negligible. Therefore it is important to know quantitatively the regions of $p_\perp$ and $2p_\perp/\sqrt{s}$ where the leading logarithmic approximation is valid.

Another specific feature of γγ scattering is the appearance of the QED log factor at both the QED vertices in second or higher order of $g^2/4\pi$*. As in higher order the 1/log factor of α_s cancels against the log factors coming from collinear transitions $\gamma \to q\bar{q}$ or $q \to gq$, we obtain a scale invariant answer and O(1) corrections [2, 12]. Increasing $p_\perp$, however, all of these corrections are suppressed since they are folded with "photon wave functions" which are soft at $x = 1$. Therefore, at large $p_\perp$, the leading order contribution will be dominant.

4.2. NUMERICAL EVALUATION OF $\sigma(e^+e^- \to e^+e^- q\bar{q}(g), p_\perp^{jet} > p_\perp^{min})$

From the discussion of the mass singularities it is clear that at very large $p_\perp$ the cross section is dominated by the Born term ($\gamma\gamma \to q\bar{q}$) and we can have a clean determination of $R_{\gamma\gamma}$. With increasing $p_\perp$ the remaining small positive corrections further decrease.

With the help of the complete $O(\alpha_s)$ corrections [eqs. (3.19) and (4.2)] we can determine quantitatively the kinematical region where the suppression becomes efficient and we can study its sensitivity to the variation of the value of the cut-off parameter M_c.

We have found very convenient to consider the total cross section $\sigma_c(e^+e^- \to e^+e^- q\bar{q}(g), p_\perp^{jet} > p_\perp^{min})$, where $p_\perp^{jet}$ is defined as

$$p_\perp^{jet} = \max\{p_\perp^q, p_\perp^{\bar{q}}, p_\perp^g\}.$$

Experimentally this requires the measurement of the transverse momenta of the hadrons and a subsequent determination of an axis $\boldsymbol{n}$ which is chosen to maximize the sum $\Sigma_i \boldsymbol{p}_{i\perp} \cdot \boldsymbol{n}$ over the corresponding semicircle. The transverse momentum of the inclusively produced jet is given by the vectorial sum $\Sigma \boldsymbol{p}_{i\perp}$ over the same semicircle. The cross section of the events with transverse momenta $p_\perp^{jet} > p_\perp^{min}$ is given by $\sigma_c(e^+e^- \to e^+e^- q\bar{q}(g), p_\perp^{jet} > p_\perp^{min})$.

We calculate the cross section σ_c at two different energies $\sqrt{s} = 30$ and 180 GeV, for various values of $p_\perp^{min}$ and M_c. The results are given in table 3, while some details of the calculation are presented in appendix B. All the cross-section values have been calculated in units of $R = 4\pi\alpha^2/3s$. σ_0 denotes the Born cross section, σ^1 is the

* In the LLA the corrections can be interpreted as contributions of large $p_\perp$ quark-quark scattering

TABLE 3
Cross-section values for ($e^+e^- \to e^+e^-, p_\perp^{jet} > p_\perp^{min}$) at $\sqrt{s} = 30$ and 180 GeV for various $p_\perp^{min}$ and M_c

	$\sqrt{s} = 30$ GeV, $\sigma_{\mu\mu} = 96$ pbarn				$\sqrt{s} = 180$ GeV, $\sigma_{\mu\mu} = 2.68$ pbarn			
	$p_\perp^{min} = 4$ GeV	$p_\perp^{min} = 6$ GeV	$p_\perp^{min} = 8$ GeV	M_c(GeV)	$p_\perp^{min} = 12$ GeV	$p_\perp^{min} = 18$ GeV	$p_\perp^{min} = 24$ GeV	$p_\perp^{min} = 36$ GeV
$\sigma^1/\sigma_{\mu\mu}$	0.062	0.0062	0.00047	0.3	1.36	0.30	0.084	0.012
	0.037	0.0037	0.00019	0.5	1.30	0.26	0.83	0.010
	0.017	0.00080		0.8	1.11	0.25	0.074	0.085
$\frac{\sigma^0+\sigma^1}{\sigma^0}$	1.39	1.21	1.073	0.3	1.56	1.48	1.38	1.30
	1.23	1.13	1.029	0.5	1.53	1.42	1.38	1.26
	1.11	1.028		0.8	1.46	1.39	1.33	1.21
σ^1/σ_1^{WW}	0.99	0.65	0.27	0.3	1.11	1.08	0.95	0.90
	0.74	0.47	0.13	0.5	1.23	1.08	1.06	0.84
	0.25	0.13		0.8	1.22	1.15	1.11	0.80
$\sigma^0/\sigma_{\mu\mu}$	0.16	0.029	0.0064		6.45	1.68	0.59	0.11

σ^1 denotes the $O(\alpha_s)$ corrections, σ_1^{WW} is its Weizsacker-Williams approximation and σ^0 is the Born cross section. σ^1 has 5–10% integration error σ^0 and σ_1^{WW} are calculated with an accuracy better than 1%

complete $O(\alpha_s)$ correction* (and σ_1^{WW} is the Weizsäcker-Williams approximation [see eqs. (4.4) and (B.16)]). We recall that cross-section values smaller than 0.1 units of R appear inaccessible experimentally at PETRA, PEP and LEP energies.

At $\sqrt{s} = 30$ GeV either the M_c dependence is strong or the cross section is too small ($p_\perp > 8$ GeV). So we conclude that at PETRA energies a clean experimental determination of $R_{\gamma\gamma}$ is extremely difficult. It would require a better understanding of the non-leading contributions.

At $\sqrt{s} = 180$ GeV, we have much smaller sensitivity to the value of M_c and the cross section is still quite large. At LEP energies for transverse moments $p_\perp^{jet} > 12$ GeV it might be possible to determine experimentally R with an accuracy of $\simeq 30\%$**.

We remark that with increasing $p_\perp$ the suppression of the complete correction σ^1 is more efficient than the suppression of σ_1^{WW}. It can be easily understood. The equivalent photon spectrum gives large weights to configurations, where the jets are produced at large angles and are almost collinear. In this case the cross section $\sigma(\gamma\gamma \to q\bar{q})$ gets large and negative first-order corrections. As $p_\perp$ is increased, this negative contribution enhances the rate of the suppression of the large positive $O(\ln(p_\perp^2/M_c^2))$ corrections.

For completeness we remark that the cross-section values presented in table 3 have been calculated using the formula (B.20) with $F^{(0)}$, $F^{(1)}$, $F_{WW}^{(1)}$ defined by eqs. (B.3), (B.19), (B.16). The errors of the numerical integration are $\simeq 5-10\%$ for σ^1 and 1% for σ^0 and σ_1^{WW}. The log factor $\ln\eta$ appearing in eq. (1.1) was defined as $\ln\eta = \ln s/4m_e^2$.

5. Conclusions

The quantity $R_{\gamma\gamma}$ can in principle be measured in three kinds of $\gamma\gamma$ processes: two large $p_\perp$ electrons, one large $p_\perp$ electron or only large $p_\perp$ hadrons. We considered the last possibility.

For the last possibility one has real $\gamma\gamma$ scattering into hadrons. When the $q\bar{q}$ production is dominant in this process, a measurement of $R_{\gamma\gamma}$ can be made. However, it has been pointed out that there are important other processes besides $q\bar{q}$ production [1] such as three- or four-jet production and non-perturbative effects. We made attempts to calculate the complete order α_s correction to the two-jet cross section. As a first step the analogue of the Sterman-Weinberg formula was derived, which is only valid for small ε and δ. When one wants to calculate finite ε, δ effects one runs into the problem of the presence of quark mass singularities. Unlike in deep inelastic photon-photon scattering there does not exist as yet a method to circumvent this problem.

Nevertheless, one can introduce a cut-off M_c to avoid the mass singularities and one can study the dependence of the α_s correction on this cut-off and for various lab

* We used $\Lambda = 0.5$ MeV, four flavours and α_s was evaluated at $s = 4(p_\perp^{min})^2$

** Electroweak radiative corrections, however, may confuse the picture

energies. Our results are expressed in a total cross section for inclusive jet production with a certain minimum $p_\perp$. For small $p_\perp$ the correction is large and sensitive to the introduced cut-off. For larger $p_\perp$ the α_s correction becomes small, but unfortunately the lowest order cross section becomes small as well.

The α_s correction was calculated in two ways; on one hand, by using the exact $q\bar{q}g$ cross section and on the other hand using the Weizsäcker-Williams approximation for the subprocess $q\gamma \to qg$. At PETRA energies it turns out that the WW approximation is not good, whereas at LEP energies it is reasonable. Where the WW approximation gives the dominant $O(\alpha_s)$ contributions and the corrections are large, one must resum all the leading and subleading logarithmic terms up to $O(1/\ln(p_\perp^2/\Lambda^2))$.

In this kinematical region the cross section ($ee \to ee$ hadrons) is large (e.g. 6–20 units of R at $\sqrt{s} = 180$ GeV and $p_\perp^{\min} \simeq 6$–12 GeV). Therefore, the evaluation of the $O(1/\ln(p_\perp^2/\Lambda))$ correction is very important.

Appendix A

In this appendix, we want to illustrate how the integral (2.14) is evaluated. We must calculate

$$I = \int_{\beta^2}^1 \frac{dz}{z^2} \int_{(1-\sqrt{1-z})/2}^{(1+\sqrt{1-z})/2} \frac{dv}{v} f(v,z), \tag{A.1}$$

with $f(v,z)$ given by eqs. (2.16), (2.17). The indefinite integrals over v can be done exactly because of the relative simplicity of $f(v,z)$. Let the primitive function be $F(v,z)$, then inserting the upper limit, we get

$$\begin{aligned} I_U &= \int_{\beta^2}^1 \frac{dz}{z^2} F\left(\tfrac{1}{2}(1+\sqrt{1-z}),z\right) \\ &= \int_{(1+\sqrt{1-\beta^2})/2}^{1/2} dx \frac{1-2x}{4x^2(1-x)^2} F(x,4x(1-x)), \end{aligned} \tag{A.2}$$

where we introduced the new variable $x = \frac{1}{2}(1+\sqrt{1-z})$.

The analogous manipulations for the lower limit of the v-integration give

$$I_L = \int_{(1-\sqrt{1-\beta^2})/2}^{1/2} dx \frac{1-2x}{4x^2(1-x)^2} F(x,4x(1-x)); \tag{A.3}$$

hence,

$$I = I_U - I_L = -\int_{(1-\sqrt{1-\beta^2})/2}^{(1+\sqrt{1-\beta^2})/2} dx \frac{1-2x}{4x^2(1-x)^2} F(x,4x(1-x)). \tag{A.4}$$

For $\beta^2 \to 0$, it is possible to extract the contributions from (A.4) which are singular and the ones which give a finite contribution. Take, e.g. the $\ln v$ contribution arising from the $\ln a$ term in eq. (2.16):

$$-\frac{2a}{v}(1+a+ab+b^2)\ln v = \left(-\frac{z^2}{4v^3}-\frac{z}{v^2}+\frac{z^2}{8v^2}+\frac{z}{v}-\tfrac{1}{2}z\right)\ln v. \qquad (A.5)$$

Performing the integration over v, we obtain, after a decomposition in partial fractions,

$$I_{\ln v} \simeq -\int_{(\beta^2/4)(1+\beta^2/4)}^{1-\beta^2/4} dx\left\{\left[\frac{3}{2x^2}-\frac{5}{2x}-\frac{1}{2(1-x)}\right]\ln x+\frac{1}{2}\left(\frac{1}{x}-\frac{1}{1-x}\right)\ln^2 x\right.$$
$$\left.+\frac{5}{4x^2}-\frac{2}{x}+2-\frac{3}{2(1-x)}\right\}. \qquad (A.6)$$

The integrals over x can be done in the limit $\beta \to 0$, but they involve higher order polylogarithmic functions; e.g.

$$\int_0^1 \frac{dx}{1-x}\ln x = \mathrm{Li}_2(1-x)\Big|_0^1 = -\tfrac{1}{6}\pi^2,$$
$$\int_0^1 \frac{dx}{1-x}\ln^2 x = 2\zeta(3), \qquad (A.7)$$

where the dilogarithm is defined by

$$\mathrm{Li}_2(x) = -\int_0^x \frac{dt}{t}\ln(1-t), \qquad (A.8)$$

and $\zeta(3)$ is Riemann's zeta-function of argument 3. For a compilation of these polylogarithmic integrals, we refer the reader to ref. [14a]*. In this way, we find

$$I_{\ln v} \simeq \frac{4}{\beta^2}\left[-\tfrac{3}{2}\ln\frac{\beta^2}{4}-\tfrac{11}{4}\right]+\tfrac{1}{6}\ln^3\frac{\beta^2}{4}-\tfrac{5}{4}\ln^2\frac{\beta^2}{4}-2\ln\frac{\beta^2}{4}+\zeta(3)-\tfrac{1}{12}\pi^2+2, \qquad (A.9)$$

where we only retained the terms which are singular or finite for $\beta \to 0$. The other terms in eq. (2.16) give similar expressions and their sum ledas to the result of eq. (2.18). Note that the $\ln^2\beta$ terms drop out in the sum. It should be noted that it is

* For those involving four powers of logarithms in the numerator, see ref [14b]

possible to derive the exact expression for (A.4) and therefore (2.18):

$$\sigma^0\left(p_\perp > \tfrac{1}{2}\sqrt{s}\,\beta\right) = 16\pi\alpha^2 R_{\gamma\gamma}\left(\frac{\alpha}{2\pi}\ln\eta\right)^2 I,$$

$$I = \frac{1}{\beta^2}\left[-\tfrac{4}{3}\ln\frac{\beta^2}{4} - \tfrac{56}{9} + \tfrac{112}{9}a_- + \tfrac{8}{3}a_+\right] - \left(\tfrac{17}{4} - \tfrac{1}{6}\pi^2\right)\ln\frac{a_-}{a_+} - \tfrac{1}{6}\ln^3\frac{\beta^2}{4} - \frac{\beta^2}{8}\ln\frac{a_-}{a_+}$$

$$+ \tfrac{1}{3}\ln^2 a_+ \ln\left(a_+ a_-^3\right) - \tfrac{187}{36} + \tfrac{187}{18}a_- + 2\left(\mathrm{Li}_3(a_+) - \mathrm{Li}_3(a_-)\right), \tag{A.10}$$

where

$$a_\pm = \tfrac{1}{2}\left(1 \pm \sqrt{1-\beta^2}\right) \tag{A.11}$$

and the trilogarithm

$$\mathrm{Li}_3(y) = \int_0^y \frac{\mathrm{Li}_2(x)}{x}\,\mathrm{d}x, \tag{A.12}$$

with $\mathrm{Li}_3(1) = \zeta(3)$. Expanding (A.10) with respect to β^2 again gives (2.18).

Appendix B

In this appendix we give formulae which have been used in obtaining the cross section values of table 1.

B.1 CROSS-SECTION FORMULAE

The differential Born cross section can be given as

$$\frac{\mathrm{d}\sigma^0}{\mathrm{d}z^2}(\gamma\gamma \to q\bar{q}) = A^0\frac{F^0(z^2)}{z^2\sqrt{1-z^2}}, \tag{B.1}$$

where

$$z^2 = \left(2p_\perp/\sqrt{\hat{s}}\right)^2,$$

$$\sqrt{\hat{s}} = 2E_\gamma,$$

$$A^0 = \frac{\pi\alpha^2}{\hat{s}}R_{\gamma\gamma}; \tag{B.2}$$

$$F^0(z^2) = 2(2-z^2). \tag{B.3}$$

The phase-space integration

$$R=\int\frac{d^3p_1}{2p_1^0}\int\frac{d^3p_2}{2p_2^0}\int\frac{d^3k_3}{2k_3^0}\delta(k_1+k_2-p_1-p_2-k_3)$$

was carried out using the simple expression

$$\frac{dR}{dz_1^2}=\frac{\hat{s}}{32}\int_{z_1}^1\frac{dx_1}{x_1\sqrt{x_1^2-z_1^2}}\int_{1-x_1}^1 dx_2 d\varphi_1 d\varphi_2, \tag{B.4}$$

where $z_i^2=(2p_i/\sqrt{\hat{s}})^2$, $x_i=2E_i/\sqrt{\hat{s}}$, φ_2 is the azimuthal angle of $\boldsymbol{p}_2$ around the $\boldsymbol{p}_1$ direction and φ_1 is the azimuthal angle of $\boldsymbol{p}_1$ around the beam axis. The cross section for $\gamma\gamma\to q\bar{q}g$ has a form similar to eq. (B.1)

$$\frac{d\sigma}{dz_1^2}=A^1\frac{F(z_1^2)}{z_1^2\sqrt{1-z_1^2}}, \tag{B.5}$$

where

$$A^1=\frac{4\alpha_s}{3\pi}A^0, \tag{B.6}$$

$$F(z_1^2)=|M|^2 z_1^2\sqrt{1-z_1^2}\,\frac{1}{\pi^2}\frac{dR}{dz_1^2}. \tag{B.7}$$

The matrix element squared, $|M|^2$, was defined earlier by eq. (4.2).

Using eqs. (B.1) and (3.19) we can obtain the contribution of the virtual corrections, soft and collinear gluon emission

$$\frac{d\sigma^v}{dz^2}=A^1\frac{f(z^2)-8(2-z^2)\ln\delta(\ln\varepsilon+\frac{3}{4})}{z^2\sqrt{1-z^2}}, \tag{B.8}$$

where

$$f(z^2)=2(2-z^2)\left[3-\tfrac{1}{3}\pi^2+g(z^2)\right], \tag{B.9}$$

$$g(z^2)=\frac{1}{1+\cos^2\theta}\left[\left(1+\sin^4\frac{\theta}{2}\right)\ln^2\sin^2\frac{\theta}{2}+\cos^2\frac{\theta}{2}\left(2+\cos^2\frac{\theta}{2}\right)\ln\sin^2\frac{\theta}{2}\right.$$

$$\left.+(\theta\leftrightarrow\pi-\theta)\right] \tag{B.10}$$

and

$$z^2 = \sin^2\theta .$$

We also define a pole term

$$|M|^2_{\text{pole}_1} = \frac{2-z_1^2}{z_1^2\sqrt{1-z_1^2}}\,\frac{8}{\hat{s}}\,\frac{1+(1-x_3)^2}{x_3(1-x_1)}\,x_1^2|\cos\theta_1|T_1T_3, \tag{B.11}$$

where

$$T_1 = \frac{\ln\delta}{\ln[\delta(1-x_3)]}, \qquad \text{if } 1-z_1 > x_3,$$

$$T_1 = \frac{\ln\delta}{\ln[\delta x_3(1-x_3)/(1-z_1)]}, \qquad \text{if } x_3 > 1-z_1,$$

$$T_3 = 1, \qquad \text{if } 1-z_1 > \tfrac{1}{4}\delta^2,$$

$$T_3 = \frac{2\ln\varepsilon + \frac{3}{2}}{2\ln(\varepsilon/v) + 2v(1-\frac{1}{4}v)}, \qquad \text{if } \tfrac{1}{4}\delta^2 > 1-z_1,$$

$$v = \tfrac{1}{2}\left(1-\sqrt{1-4(1-z_1)/\delta^2}\right). \tag{B.12}$$

with a similar expression for the pole at $x_2 \simeq 1$. These squared matrix elements give

$$\frac{d\sigma^{\text{pole}}}{dz^2} = A^1\frac{8(2-z^2)\left[-\ln\delta\left(\ln\varepsilon+\frac{3}{4}\right)\right]}{z^2\sqrt{1-z^2}}, \tag{B.13}$$

which cancels the $\ln\delta$, $\ln\varepsilon$ dependence of eq. (B.8).

The T_1, T_2 factors in eq. (B.11) are introduced to compensate the changes in the integration region as indicated in the Dalitz plot of fig. 9. Therefore, by definition we obtain

$$\int_\varepsilon^{v \text{ or } 1} dx_3\left(\frac{2}{x_3}-2+x_3\right)\int_{\delta^2 x_3(1-x_3)}^{\min[x_3,(1-z)]}\frac{dy}{y}\,T_1T_2 = 4\ln\delta\left(\ln\varepsilon+\tfrac{3}{4}\right),$$

where $y = 1-x_1$.

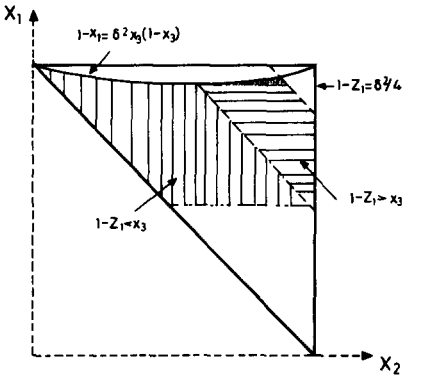

Fig 9 Dalitz plot of x_1 and x_2 illustrating the various integration regions at fixed z_1. When $1-z_1 < \frac{1}{4}\delta^2$ only the dotted area is relevant. When $1-z_1 < x_3$ the integration region is the area shaded by vertical lines, when $x_3 < 1-z_1$ it is given by the area shaded by horizontal lines.

Finally, if we use the cross-section formula

$$\frac{d\sigma}{d\cos\hat{\theta}}(q\gamma \to qg) = \frac{4\pi\alpha_s\alpha}{3\hat{s}}\left(-\frac{\hat{s}}{\hat{u}} - \frac{\hat{u}}{\hat{s}}\right), \tag{B.14}$$

the integration over x in eq. (4.4) can be carried out and we get

$$\frac{d\sigma_1^{WW}}{dz^2} = A^1 \frac{F^{WW}(z^2)}{z^2\sqrt{1-z^2}}, \tag{B.15}$$

where

$$F^{WW}(z^2) = 2\ln\frac{p_\perp^2}{M_c^2}\sqrt{1-z^2}\left[(2-3z^2+2z^4)\ln\frac{2-z^2+2\sqrt{1-z^2}}{z^2} + (4z^2-1)\sqrt{1-z^2}\right]. \tag{B.16}$$

B 2 NUMERICAL EVALUATION

In the numerical integration program, three different regions are considered:

$$\text{region (1)}: p_{\perp\bar{q}} > p_{\perp q}, p_{\perp g}, \qquad p_\perp^{max} = p_{\perp\bar{q}},$$

$$\text{region (2)}: p_{\perp q} > p_{\perp\bar{q}}, p_{\perp g}, \qquad p_\perp^{max} = p_{\perp q},$$

$$\text{region (3)}: p_{\perp g} > p_{\perp q}, p_{\perp\bar{q}}, \qquad p_\perp^{max} = p_{\perp g},$$

since the phase-space distributions dR/dz^2 are different in these regions. In order to cancel the $\ln\varepsilon\ln\delta$ singularity analytically instead of $|M|^2 dR/dz^2$ a regularized distribution has been used:

$$|M|^2_R \frac{dR}{dz^2} = \frac{1}{\pi^2}\left\{2\left[|M|^2 - |M|^2_{\text{pole}}\right]\frac{dR^{(1)}}{dz_q^2} + |M|^2\frac{dR^{(3)}}{dz_g^2} - 2|M|^2_{\text{pole}}\frac{dR^{(1)+(2)}}{dz_{\bar{q}}^2}\right\}, \tag{B.17}$$

where $dR^{(i)}/dz^2 = dR/dz^2$ in region (i), otherwise it is zero, and

$$z = \max\{z_q, z_{\bar{q}}, z_g\}.$$

The complete $O(\alpha_s)$ cross section, after cancelling the $\ln\varepsilon$, $\ln\delta$ dependence analytically can be given as

$$\frac{d\sigma^1}{dz^2} = A^1\frac{F^1(z^2)}{z^2\sqrt{1-z^2}}, \tag{B.18}$$

where

$$F^1(z^2) = f(z^2) + \frac{z^2\sqrt{1-z^2}}{\pi^2}|M|^2_R\frac{dR}{dz^2}. \tag{B.19}$$

Finally, we must fold the parton cross sections (B.1), (B.7) and (B.9) with the equivalent photon spectrum [eq. (1.1)] $N(x_q)$:

$$\frac{d\sigma}{dp_\perp^2}(s,p_\perp^2) = \int dx_a \int dx_b N(x_a)N(x_b)\frac{d\sigma}{dp_\perp^2}(x_a x_b s, p_\perp^2).$$

Introducing new variables $\tau = x_a x_b$ and $y = x_a/x_b$ the y integration can be performed and we have

$$\sigma_c^a(e^+e^-, p_\perp > p_\perp^{\min}) = \left(\frac{\alpha}{2\pi}\ln\eta\right)^2 A^a \times \int_{(2p_\perp^{\min}/\sqrt{s})^2}^1 \frac{dz^2}{z^2}\int_{z^2}^1 \frac{c(\tau)}{\tau\sqrt{\tau^2 - \tau z^2}} F^a(z^2/\tau), \tag{B.20}$$

where

$$c(\tau) = 2\left[-(2+\tau)^2\ln\tau - 4(2+\tau)(1-\tau) + 2(1-\tau^2)\right]. \tag{B.21}$$

The functions F^0, F^1, F_1^{WW} are defined by eqs. (B.3), (B.19) and (B.16). In the argument of the log factor in eq. (B.16) $(p_\perp^{min}/M_c)^2$ was used. F^1 was calculated by eq. (B.19) using $\hat{s} = s\tau$ and $p_\perp^1, p_\perp^2 > M_c$.

References

[1] F E. Low, Phys. Rev. 120 (1960) 582,
H Cheng and T T. Wu, Phys. Rev Lett 23 (1969) 1311; Phys. Rev D1 (1970) 2775

[2] S.J Brodsky, T DeGrand, J. Gunion and J Weiss, Phys Rev Lett 41 (1978) 672; Phys Rev D19 (1979) 1418

[3] F A Berends, Z Kunszt and R Gastmans, Phys Lett. 92B (1980) 186

[4] G 't Hooft and M Veltman, Nucl Phys B44 (1972) 189;
C G Bollini and J.J Giambiagi, Phys Lett 40B (1972) 566;
J F Ashmore, Nuovo Cim Lett. 4 (1972) 289;
G M Cicuta and E. Montaldi, Nuovo Cim Lett 4 (1972) 329

[5] G Sterman and S. Weinberg, Phys. Rev. Lett. 39 (1977) 1436

[6] R Gastmans, J Verwaest and R Meuldermans, Nucl Phys B105 (1976) 454

[7] R Gastmans and R Meuldermans, Nucl Phys B63 (1973) 277;
W J Marciano and A Sirlin, Nucl Phys B88 (1975) 86

[8] A C. Hearn, REDUCE 2. Users Manual, Utah (1973)

[9] F A Berends and R Gastmans, *in* Electromagnetic interactions of hadrons, ed A Donnachie and G Shaw (Plenum, 1978), vol. 2, p 471

[10] F A Berends and R Gastmans, ref [10], p 481 and p 483

[11] F A Berends, R Gastmans and T T Wu, Univ of Leuven preprint KUL-79/022

[12] C Llewellyn-Smith, Phys Lett 79B (1978) 83

[13] E Witten, Nucl Phys B120 (1977) 189;
W A Bardeen and A J. Buras, Phys. Rev. D20 (1979) 166

[14] (a) R Barbieri, J A Mignaco and E Remiddi, Nuovo Cim. 11A (1972) 824,
(b) R Gastmans and W Troost, University of Leuven preprint KUL-TF-80/10, to be published in Simon Stevin